




RESEARCH ARTICLE

Proteomic analysis identifies HSP90AA1, PTK2B, and ANXA2 in the human entorhinal cortex in Alzheimer's disease: Potential role in synaptic homeostasis and A β pathology through microglial and astroglial cells

Veronica Astillero-Lopez^{1,2} | Sandra Villar-Conde^{1,2} | Melania Gonzalez-Rodriguez^{1,2} | Alicia Flores-Cuadrado^{1,2} | Isabel Ubeda-Banon^{1,2}  | Daniel Saiz-Sanchez^{1,2}  | Alino Martinez-Marcos^{1,2} 

¹Neuroplasticity and Neurodegeneration Laboratory, CRIB, Ciudad Real Medical School, University of Castilla-La Mancha (UCLM), Ciudad Real, Spain

²Grupo de Neuroplasticidad y Neurodegeneración, Instituto de Investigación Sanitaria de Castilla-La Mancha (IDISCAM), Castilla-La Mancha, Spain

Correspondence

Daniel Saiz-Sanchez and Isabel Ubeda-Banon, Neuroplasticity and Neurodegeneration Laboratory, CRIB, Ciudad Real Medical School, University of Castilla-La Mancha (UCLM), Ciudad Real, Spain.
Email: daniel.saiz@uclm.es and isabel.ubeda@uclm.es

Funding information

Ministerio de Ciencia e Innovación, Grant/Award Number: PID2019-108659RB-I00; Autonomous Government of Castilla-La Mancha/ERDF, Grant/Award Numbers: SBPLY/17/180501/000430, SBPLY/21/180501/000093; UCLM/ERDF, Grant/Award Number: 2022-GRIN-34200

Abstract

Alzheimer's disease (AD), the most prevalent neurodegenerative disorder worldwide, is clinically characterized by cognitive deficits. Neuropathologically, AD brains accumulate deposits of amyloid- β (A β) and tau proteins. Furthermore, these misfolded proteins can propagate from cell to cell in a prion-like manner and induce native proteins to become pathological. The entorhinal cortex (EC) is among the earliest areas affected by tau accumulation along with volume reduction and neurodegeneration. Neuron–glia interactions have recently come into focus; however, the role of microglia and astroglia in the pathogenesis of AD remains unclear. Proteomic approaches allow the determination of changes in the proteome to better understand the pathology underlying AD. Bioinformatic analysis of proteomic data was performed to compare ECs from AD and non-AD human brain tissue. To validate the proteomic results, western blot, immunofluorescence, and confocal studies were carried out. The findings revealed that the most disturbed signaling pathway was synaptogenesis. Because of their involvement in synapse function, relationship with A β and tau proteins and interactions in the pathway analysis, three proteins were selected for in-depth study: HSP90AA1, PTK2B, and ANXA2. All these proteins showed colocalization with neurons and/or astroglia and microglia and with pathological A β and tau proteins. In particular, ANXA2, which is overexpressed in AD, colocalized with amoeboid microglial cells and A β plaques surrounded by astrocytes. Taken together, the evidence suggests that unbalanced expression of HSP90AA1, PTK2B, and ANXA2 may play a significant role in synaptic homeostasis and A β pathology through microglial and astroglial cells in the human EC in AD.

KEYWORDS

amyloid- β , ANXA2, astroglia, GFAP, IBA1, microglia, neurodegeneration, PYK2, synapse, tau

1 | INTRODUCTION

Alzheimer's disease (AD) is the most prevalent neurodegenerative disorder worldwide, and its prevalence is

rapidly growing owing to the aging population [1]. This disease is clinically characterized by cognitive deficits and memory dysfunction. Neuropathologically, deposits of amyloid- β (A β) and tau proteins are found in AD

This is an open access article under the terms of the [Creative Commons Attribution-NonCommercial](https://creativecommons.org/licenses/by-nc/4.0/) License, which permits use, distribution and reproduction in any medium, provided the original work is properly cited and is not used for commercial purposes.

© 2024 The Authors. *Brain Pathology* published by John Wiley & Sons Ltd on behalf of International Society of Neuropathology.

brains [2]. These misfolded proteins can act in a prion-like manner, propagating from cell to cell through neurons and/or glial cells and inducing native proteins to become pathological [3, 4]. Accumulating evidence points to a prominent role of astroglia and microglia in AD pathogenesis [5]. However, whether both glial cell populations facilitate the clearance [6, 7] and/or the spread [8–10] of A β and tau pathological proteins remains unclear.

Since tau accumulation occurs in a predictable manner, six neuropathological stages have been established for AD [11]. Along with the locus coeruleus, the entorhinal cortex (EC) is one of the earliest areas involved in tauopathy (Braak stage I). From the EC, tau aggregates spread out from within the medial temporal lobe to the rest of the cortex. Importantly, the EC is the principal entrance of cortical information into the hippocampus through the perforant pathway [12]. Because of its unique location in the cortico-hippocampal circuit, the EC constitutes an essential connectomic hub [13] for memory encoding, consolidation, and retrieval [14, 15]. In fact, medial temporal lobe atrophy, especially in the hippocampus and EC, is one of the hallmarks of AD and is used as a diagnostic criterion [16].

Neuronal loss and volume reduction in the EC have been widely reported [17, 18]. There is a clinical need to identify diagnostic biomarkers and therapeutic strategies to protect against EC degeneration. Determining changes in the proteome is a potential tool to better understand the pathology underlying AD [19–22]. Studies applying proteomic approaches to the human EC have been scarce, but have identified alterations related to protein phosphorylation [23] and ion transport function [24] in patients with AD. A recent proteomic study revealed an interesting profile of upregulated (S100A6, PPP1R1B, BAG3, and PRDX6) and downregulated (GSK3B, SYN1, DLG4, and RAB3A) proteins related to neurodegeneration and astrogliosis in the human EC in AD [18].

In this study, a bioinformatic analysis of proteomic data was performed in the EC in AD. Heat shock protein HSP 90-alpha (HSP90AA1), protein-tyrosine kinase 2-beta (PTK2B), and annexin-2 (ANXA2) were selected because of their involvement in synaptic function, their potential interaction with A β and tau pathological proteins, and their connections in the pathway analysis. Finally, we thoroughly analyzed the specific expression patterns of these proteins in neurons, astroglia, and microglia to disentangle cell-type-specific contributions to disease pathology.

2 | METHODS

2.1 | Human samples

Postmortem human brain samples were provided by the *Institut d'Investigacions Biomèdiques August Pi i Sunyer*

(*IDIBAPS*), *Biobanco en Red de la Región de Murcia* (*BIOBANC-MUR*), *Biobanco de Tejidos de la Fundación CIEN* (*BTCIEN*), and *Biobanco del Principado de Asturias* (*BPA*), which are integrated in the Spanish National Biobanks Network. The samples were then processed following standard operating procedures with the approval of the Clinical Research Ethics Committee of Ciudad Real University Hospital (PID2019-108659RBI00). Two experimental groups were used: $N = 12$ non-AD cases and $N = 12$ AD cases neuropathologically diagnosed with Braak stages V or VI. Fresh frozen tissue from five cases per experimental group were used to perform protein extraction and western blotting (mean age \pm standard error of the mean [SEM]: 75.60 ± 3.265 , $n = 5$ non-AD; 78.60 ± 5.085 , $n = 5$ AD; p value = 0.793). Formalin-fixed tissue from the seven other cases per experimental group were used for histological procedures, colocalization studies, and fluorescence quantification (mean age \pm SEM: 67.80 ± 6.224 , $n = 5$ non-AD; 80.20 ± 3.056 , $n = 5$ AD; p value = 0.396). Information about the cases used is detailed in Table 1.

To standardize sample conditions from different brain banks, all formalin-fixed tissues were postfixed by immersion in 4% paraformaldehyde. For cryoprotection, blocks were submerged in a phosphate-buffered (PB) solution of 2% dimethyl sulfoxide (DMSO) and 10% glycerol for 48 h and then in a PB solution of 2% DMSO and 20% glycerol for 48 h. Later, tissue was cut with a freezing sliding microtome into a series of 50- μ m-thick coronal sections. The first series was used for Nissl staining. The remaining series were stored in cryoprotective solution and kept at -20°C until further processing.

2.2 | Proteomic data analysis

The human EC proteins data analyzed in the present investigation (Dataset S1a) come from a proteomic study previously reported by our group [18]. Briefly, global protein profiles were obtained by sequential window acquisition of all theoretical fragment ion spectra mass spectrometry (SWATH-MS) and were analyzed using data-dependent acquisition shotgun nanoscale liquid chromatography coupled to tandem mass spectrometry (nanoLC-MS/MS) runs. The mass spectrometry proteomics data are available in the ProteomeXchange Consortium (<http://proteomecentral.proteomexchange.org>) via the PRIDE partner repository with the dataset identifier PXD029359.

Prior to the bioinformatics analysis of proteomic data, Excel was used to normalize protein abundance by log transformation and to filter according to fold change and/or p value. After an unpaired two-tailed t test was applied, differentially expressed proteins (DEPs) were defined as those that met a p value threshold < 0.01 and a fold change threshold of ≥ 1.8 for upregulation or ≤ 0.55 for downregulation.

TABLE 1 Demographic and clinic-pathological features of the individuals used in this study.

Case	DxAP	Assay	Braak stage	Sex	Age (years)	PMD (hh:mm)	Brain weight (g)	Original fixation	Cause of death
1	AD	IF	VI	F	87	15:30	990	Formaldehyde	Sepsis
2	AD	IF, Q	V	F	80	4:00	910	Formaldehyde	Respiratory infection
3	AD	IF	VI	F	85	2:00	1150	Formaldehyde	Cardiorespiratory arrest
4	AD	IF, Q	VI	M	77	5:00	1330	Formaldehyde	Sepsis of bacterial origin
5	AD	IF, Q	VI	M	77	6:00	1060	Formaldehyde	Acute respiratory infection
6	AD	IF, Q	V	M	75	3:00	1050	Formaldehyde	Multi-organic failure
7	AD	IF, Q	VI	M	92	6:00	960	Formaldehyde	n.a.
8	AD	WB	VI	M	90	4:30	1070	Frozen no-fix	Cardiorespiratory arrest
9	AD	WB	V-VI	F	91	5:00	n.a.	Frozen no-fix	n.a.
10	AD	WB	VI	F	76	11:10	900	Frozen no-fix	Cardiorespiratory arrest
11	AD	WB	VI	M	69	2:25	n.a.	Frozen no-fix	Multi-organic failure
12	AD	WB	VI	F	67	4:15	n.a.	Frozen no-fix	Bronchopneumonia
13	NAD	IF	n.a.	F	75	10:30	1050	Formaldehyde	Cardiogenic shock
14	NAD	IF, Q	II	F	81	5:00	1100	Formaldehyde	Multi-organic failure
15	NAD	IF	II	F	62	2:00	1050	Formaldehyde	Cardiorespiratory arrest
16	NAD	IF, Q	II	M	84	3:00	1400	Formaldehyde	Cardiorespiratory arrest
17	NAD	IF, Q	I	M	53	5:00	1300	Formaldehyde	Cardiorespiratory arrest
18	NAD	IF, Q	I	M	58	6:00	1500	Formaldehyde	Acute myocardial infarction
19	NAD	IF, Q	I	M	63	2:00	1400	Formaldehyde	Cardiorespiratory arrest
20	NAD	WB	II	F	83	7:20	1320	Frozen no-fix	Intestinal ischemia
21	NAD	WB	n.a.	M	77	10:31	n.a.	Frozen no-fix	n.a.
22	NAD	WB	n.a.	M	68	4:10	1350	Frozen no-fix	Sepsis
23	NAD	WB	n.a.	F	82	4:00	800	Frozen no-fix	Respiratory failure
24	NAD	WB	n.a.	M	68	4:00	1220	Frozen no-fix	Cardiorespiratory arrest

Abbreviations: AD, Alzheimer's disease; DxAP, neuropathological diagnosis; F, Female; IF, Immunofluorescence; M, Male; n.a., not available; NAD, non-Alzheimer's disease; PMD, post-mortem delay; Q, Quantification; WB, Western Blot.

2.3 | Bioinformatic analysis

Interactome and pathway analyses were performed using QIAGEN's machine learning-based bioinformatic tool Ingenuity Pathway Analysis (IPA, QIAGEN Redwood City, www.qiagen.com/ingenuity). SYNGO (Synaptic Gene Ontologies, <https://syngoportal.org/>) was applied to analyze synapse function. BioGRID 4.4 (a database of protein, genetic, and chemical interactions, <https://thebiogrid.org/>) was consulted as a repository of protein interactions with pathological markers (APP and MAPT). Finally, Venn diagrams of the data were constructed using Venny (<https://bioinfopg.cnb.csic.es/tools/venny/>).

2.4 | Protein extraction and western blotting

Frozen tissue samples (Table 1) were disrupted with a pellet pestle (Sigma-Aldrich) and homogenized in ice-cold radioimmunoprecipitation assay (RIPA) buffer

(50 mM Tris-HCl pH 7.4, 150 mM NaCl, 0.1% Triton X-100, 0.1% SDS, 0.5% Na-deoxycholate) with a protease inhibitor cocktail (Sigma-Aldrich). Homogenates were then shaken for 2 h at 4°C, followed by centrifugation at 12,000g for 5 min at 4°C. Subsequently, supernatants were collected. Protein concentration was determined using a Bicinchoninic Acid Kit for Protein Determination (Sigma-Aldrich) and a Multiskan FC Microplate Photometer (Thermo Fisher Scientific).

Equal amounts of lysate proteins (30 µg) from human samples (Table 1) were loaded onto 10% polyacrylamide gels for SDS-PAGE and electrophoretically transferred to nitrocellulose (HSP90AA1) or PVDF (ANXA2 and PTK2B) membranes. All values were normalized to the housekeeping protein GAPDH. The membranes were blocked with nonfat dry milk in TTBS (0.1% Tween-20, 0.06 M NaCl, and 0.2 M Tris-hydroxymethyl-aminomethane pH 8.8) for 1 h and incubated with primary antibodies (Table 2) overnight at 4°C. The membranes were then washed with TTBS and incubated with the appropriate peroxidase-conjugated secondary antibodies (1:5000). Band

TABLE 2 Details of antibodies used in this study.

Antigen	Manufacturer	Catalog n°	Species	Assay	Dilution	Blocking buffer	Secondary antibody
Iba-1	Abcam	ab5076	Goat polyclonal	IF	1:1000	TBS + 0.3% TX-100 + 10% NDS	Alexa Fluor® 647 donkey
GFAP	Abcam	ab53554	Goat polyclonal	IF	1:500	TBS + 0.3% TX-100 + 10% NDS	Alexa Fluor® 647 donkey
β-Amyloid	Cell Signaling	2454	Rabbit polyclonal	IF	1:250	PBS + 0.3% TX-100 + 2% NDS	Alexa Fluor® 488 donkey
β-Amyloid	Cell Signaling	2450	Mouse monoclonal	IF	1:1000	TBS + 0.3% TX-100 + 10% NDS	Alexa Fluor® 568 donkey
Tau	Cell Signaling	46,687	Rabbit monoclonal	IF	1:100	PBS + 0.3% TX-100	Alexa Fluor® 488 donkey
Tau	Cell Signaling	4019	Mouse monoclonal	IF	1:800	TBS + 0.3% TX-100 + 10% NDS	Alexa Fluor® 568 donkey
Neuro-Chrom™ Pan Neuronal	Sigma–Aldrich	MAB2300	Mouse monoclonal	IF	1:100	TBS + 0.3% TX-100 + 10% NDS	Alexa Fluor® 568 donkey
ANXA2	Abcam	ab41803	Rabbit polyclonal	IF; WB	1:100; 1:1000	TBS + 0.3% TX-100 + 10% NDS; milk 5%	Alexa Fluor® 488 donkey; polyclonal goat immunoglobulins/HRP
HSP90α	Invitrogen	MA3-010	Mouse monoclonal	IF; WB	1:20; 1:500	TBS + 0.3% TX-100 + 10% NDS; milk 5%	Alexa Fluor® 568 donkey; goat IgG (H + L) HRP-conjugated
PYK2	Abcam	ab32571	Rabbit monoclonal	IF; WB	1:100; 1:2000	TBS + 0.3% TX-100 + 10% NDS; milk 5%	Alexa Fluor® 488 donkey; polyclonal goat immunoglobulins/HRP
GAPDH	Cell Signaling	2118	Rabbit monoclonal	WB	1:2000	Milk 5%	Polyclonal goat immunoglobulins/HRP

Abbreviations: IF, Immunofluorescence; PBS, phosphate-buffered saline; TBS, tris-buffered saline; WB, Western Blot.

intensity was imaged with a Syngene G:Box (GeneSys software) after incubation with Enhanced Chemiluminescence reagents (Thermo Fisher Scientific) and analyzed with ImageJ.

2.5 | Immunofluorescence

For immunofluorescence, epitopes from formaldehyde-fixed human samples (Table 1) were unmasked by boiling tissue sections under pressure for 2 min in citrate buffer. After this unmasking step, the sections were immersed in formic acid for 3 min and rinsed in phosphate-buffered saline (PBS) or tris-buffered saline (TBS; 0.05 M NaCl, 0.05 M Tris, HCl pH 7.6). Endogenous peroxidase activity was inhibited using 1% H₂O₂ for 20 min. Tissue was

then immersed in blocking buffer for 30 min at room temperature and incubated overnight at 4°C with primary antibodies (for details, see Table 2). Then, sections were incubated for 2 h at room temperature with Alexa Fluor 488, 568, or 647 antibodies against multiple species (1:200 in TBS with 0.3% Triton X-100; Invitrogen), counterstained with DAPI (0.01% in TBS, Sigma–Aldrich) for 5 min in the dark, and coverslipped with PVA-DABCO (Sigma–Aldrich).

2.6 | Quantification of fluorescence intensity

Labeling of HSP90AA1, PTK2B, and ANXA2 markers was stereologically quantified in 10 cases (5 non-AD and 5 AD cases, for details see Table 1). Sections from levels

16.0 to 23.9 mm from bregma were selected [25]. This method included random point selection in the EC, photography, and confocal microscopy analysis.

Briefly, the EC was outlined on immunofluorescence-stained slides by consulting parallel Nissl-stained slides. We performed an unbiased protocol: first, a transparent millimetric grid was randomly overlapped with the slide, and the crossing points of the grid were used to select the points on the slide to take the pictures. Second, three tissue sections per case were selected, and three random images per section were captured with a Zeiss LSM 800 confocal microscope using a 20× objective (Plan-Apochromat 20×/0.8 M27). Third, images (HSP90AA1, $n = 90$; PTK2B, $n = 90$; and ANXA2, $n = 90$) were analyzed with Zen blue 3.3 software supplied by Carl Zeiss. The same conditions and parameters of background and threshold were maintained between non-AD and AD cases for each channel. The mean intensity value of each image was measured with the graphics tool of Zen software. The total fluorescence signal intensity was quantified as the average across labeled pictures for each case.

2.7 | Colocalization studies

Double or triple immunofluorescence staining of selected proteins with microglial (IBA1), astroglial (GFAP) or neuronal (PAN) markers and A β and tau pathological markers was analyzed with a Zeiss LSM 800 confocal microscope coupled to Zen blue 3.3 software. Spatial colocalization was analyzed using high-magnification images and z-stacks obtained with a 40× objective (Plan-Apochromat 40×/0.95 Korr M27) and a 63× objective (Plan-Apochromat 63×/1.40 Oil DIC M27).

2.8 | Statistics

All statistical analyses were conducted using GraphPad Prism 6 Software (GraphPad Inc., San Diego, CA, USA, v.6). Data are expressed as the mean \pm SD, and statistical comparisons were made using t tests or Mann–Whitney U tests for normally or nonnormally distributed data, respectively. The statistical significance level was set at $\alpha = 0.05$.

3 | RESULTS

3.1 | Synaptogenesis is the most disturbed signaling pathway in the EC

Starting from a total of 1635 identified proteins in the human EC, the number of DEPs was 139, with 52 upregulated and 87 downregulated proteins (Dataset S1b). Ingenuity Pathway Analysis was used to investigate the potential implications of the observed changes in

metabolic pathways and protein interaction networks. The analysis of the top 10 canonical pathways revealed that the synaptogenesis signaling pathway had the largest negative z score (Figure 1A). Inhibited functions relevant to this pathway include the growth and branching of neurites through the upstream regulator PPARA (peroxisome proliferator-activated receptor alpha); when these functions are inhibited, organismal death results (Figure 1B). More specifically, annotations of the increased and decreased functions related to synapses are shown in Figure 1C, where a substantial reduction in the growth and branching of neurites is highlighted (Dataset S1c).

To further analyze synaptic homeostasis, we performed a SYNGO analysis, for which cellular component and biological process enrichment analysis in synapses revealed that 37/139 DEPs were involved (Dataset S1d). The synapse Gene Ontology (GO) term (GO:0045202) revealed nine specific proteins (AP2M1, ARHGDI, CORO1A, CYFIP2, EEF1A2, FGA, RPLP2, RPS25, TBC1D24; p value = $8.97e-12$). There were relevant alterations on both the presynapse (GO:0098793), with seven altered proteins (AP1G1, CADPS, PFN2, PRKACA, PTK2B, SCRNI, SYNJ1; p value = $4.12e-6$), and the postsynapse (GO:0098794), with six altered proteins (ACTR2, CYFIP1, PFN2, PPP1R1B, PRKACA, and PTK2B; p value = $1e-4$). PTK2B, affected on both the presynapse and postsynapse, was also involved in the postsynaptic density (GO:0099092), postsynaptic modulation of chemical synaptic transmission (GO:0099170) and regulation of postsynaptic density assembly (GO:0099151) (Dataset S1e,f).

3.2 | Interrelationship between DEPs and A β and tau pathological proteins

To determine how many of the DEPs were related to pathological A β (APP) and tau (MAPT) proteins, we generated a Venn diagram using the list of interacting proteins from BioGRID (Figure 1D). Sixteen proteins matched A β (APP), and 20 matched tau (MAPT), of which only 3 were common (GSK3B, HSP90AA1, and PPIA).

To characterize the AD-affected human EC in detail, proteomic data were functionally analyzed (Figure 1E). Several direct and indirect interactions between A β (APP) and DEP proteins were noted when APP was incorporated into the interactome map. Specifically, 8 increased proteins (AHNAK, AIF1, ANXA2, H2AZ2, H4C1, LMNA, MYL12A, and PRDX6) and 14 decreased proteins (ACOT7, ARMT1, COPS2, DLG4, EPB41L3, GSK3B, HSP90AA1, PHYHIPL, PPIA, PRKACA, PTK2B, RAN, RASAL1, and TPP2) were involved. The remarkable pattern of AIF1 (a synonym of IBA1), related to microglial cells, is shown in the interactome map.

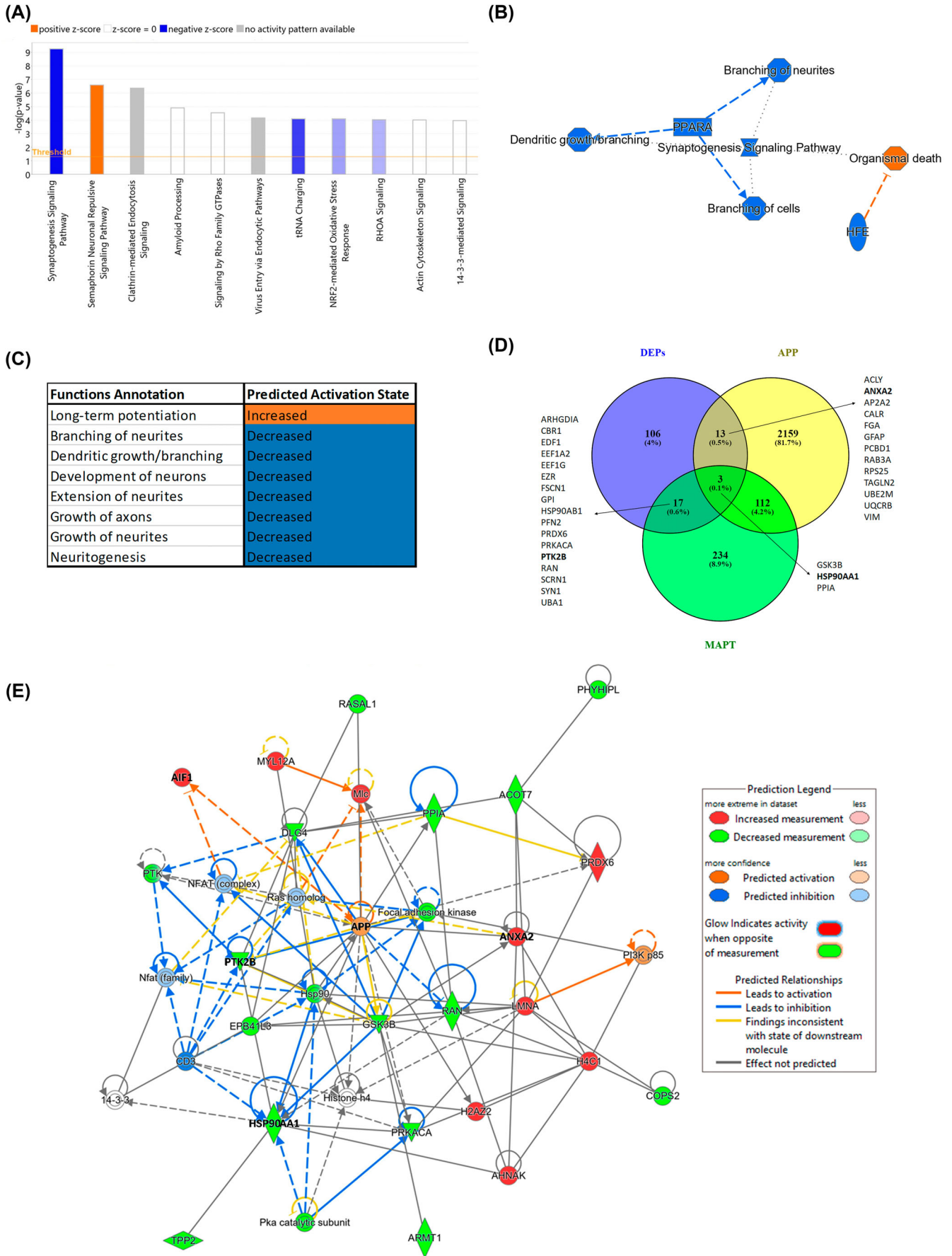


FIGURE 1 Legend on next page.

3.3 | Proteomic analysis reveals HSP90AA1, PTK2B, and ANXA2 as proteins of interest in AD pathology

After bioinformatic analyses of proteomic data, three proteins were selected (two downregulated, HSP90AA1 and PTK2B, and one upregulated, ANXA2) for further experiments based on different criteria. The first criterion was statistical significance based on the p value (<0.01) and fold change (≥ 1.8 for upregulated and ≤ 0.55 for downregulated expression) established to select DEPs. Second, the three proteins were selected based on their interactions with A β and/or tau protein extracted from the BioGRID analysis. More specifically, ANXA2 was related to A β , PTK2B was related to tau, and HSP90AA1 was related to both. Third, all three proteins showed direct or indirect functional interactions with A β protein and microglia in an interactome map. Moreover, PTK2B was also selected due to its known involvement in altered synapses in AD.

3.4 | ANXA2 expression is increased in the EC in AD

HSP90AA1, PTK2B, and ANXA2 protein levels were quantified in non-AD and AD cases using western blotting. No statistically significant differences were found in HSP90AA1 (p value = 0.5317), PTK2B (p value = 0.0952), or ANXA2 (p value = 0.4127) (Figure S1A–C, respectively). All proteins showed a trend consistent with the proteomic data analysis, but the trend was not statistically significant, probably due to the variability among human samples.

In addition to western blotting, we performed immunofluorescence analysis to check the downregulation or upregulation of proteins of interest. The expression of HSP90AA1 (Figure 2A–C), PTK2B (Figure 2D–F), and ANXA2 (Figure 2G–I) in the EC was investigated in non-AD and AD cases via confocal microscopy. No significant differences were found in HSP90AA1 (Figure 2C; Mann–Whitney $U = 4$, p value = 0.0952) or PTK2B (Figure 2F; Mann–Whitney $U = 12$, p value = 0.9444) labeling. On the other hand, statistical analysis demonstrated a significant increase in ANXA2 labeling in AD compared to non-AD cases (Figure 2I; Mann–Whitney $U = 0$, p value = 0.0079) in the EC.

3.5 | HSP90AA1, PTK2B, and ANXA2 colocalize with glial cells and pathological protein aggregates

Immunofluorescence analysis of selected proteins with microglial (IBA1), astroglial (GFAP), or neuronal (PAN) markers was performed to assess spatial relationships. In addition, the pathological markers A β and tau were investigated together with HSP90AA1, PTK2B, and ANXA2.

HSP90AA1 colocalized with microglial (Figure 3A–C) and astroglial (Figure 3D–F) cells in AD. Moreover, HSP90AA1 was found in the vicinity of A β plaques (Figure 3G–I) and colocalized with tau (Figure 3J–L) deposits in AD cases. PTK2B colocalized with neurons (Figure 4A–C) and was found inside microglial cells (Figure 4D–F). Furthermore, PTK2B colocalized with A β (Figure 4G–I) and tau (Figure 4J–L) deposits in AD cases. ANXA2 overlapped with microglial (Figure 5A–C) and astroglial (Figure 5D–F) cells. Moreover, ANXA2 showed an intense relationship with A β plaques (Figure 5G–I, Movie S1).

3.6 | Increased ANXA2 expression is associated with A β plaques surrounded by astrocytes and amoeboid microglial cells

Concerning the increase of ANXA2 in the EC in AD, we further studied its interactions with A β plaques and glial cells. We observed astrocytes specifically around A β plaques that coexpressed ANXA2 (Figure 6). Interestingly, triple colocalization of ANXA2, HSP90AA1, and IBA1 was observed in microglial cells with an amoeboid morphology but not in those with a ramified morphology (Figure 7, arrows and arrowheads, respectively).

4 | DISCUSSION

This study constitutes an exploratory data analysis of DEPs in the EC in AD. The limitations establishing homogeneous study groups in terms of age, Braak tau stage, and region has reduced the number of samples used for the DEPs validation. Despite the sample size limitation, this is a novel approach to using DEPs from proteomic datasets to then apply those discoveries back to AD and non-AD tissues. In addition, the exploratory finding that

FIGURE 1 Proteomic analysis of the human EC in AD. (A) The top 10 canonical pathways classified by z score. (B) Graphical summary of the synaptogenesis signaling pathway, the top canonical pathway, with the associated functions and the upstream regulators. (C) Increased and decreased functions related to synapses. (D) Common and unique DEPs related to AD pathology. Venn diagram showing the overlap between DEPs and pathological A β (APP) and/or tau (MAPT) proteins. Gene names are indicated for the corresponding overlapping areas of interest. (E) Representative functional protein interactome map for DEPs and APP. The proteins selected in this study (HSP90AA1, PTK2B, and ANXA2) and those related to microglial cells (AIF1) and A β (APP) pathology are highlighted in bold. A β , amyloid- β ; AD, Alzheimer's disease; DEPs, differentially expressed proteins; EC, entorhinal cortex.

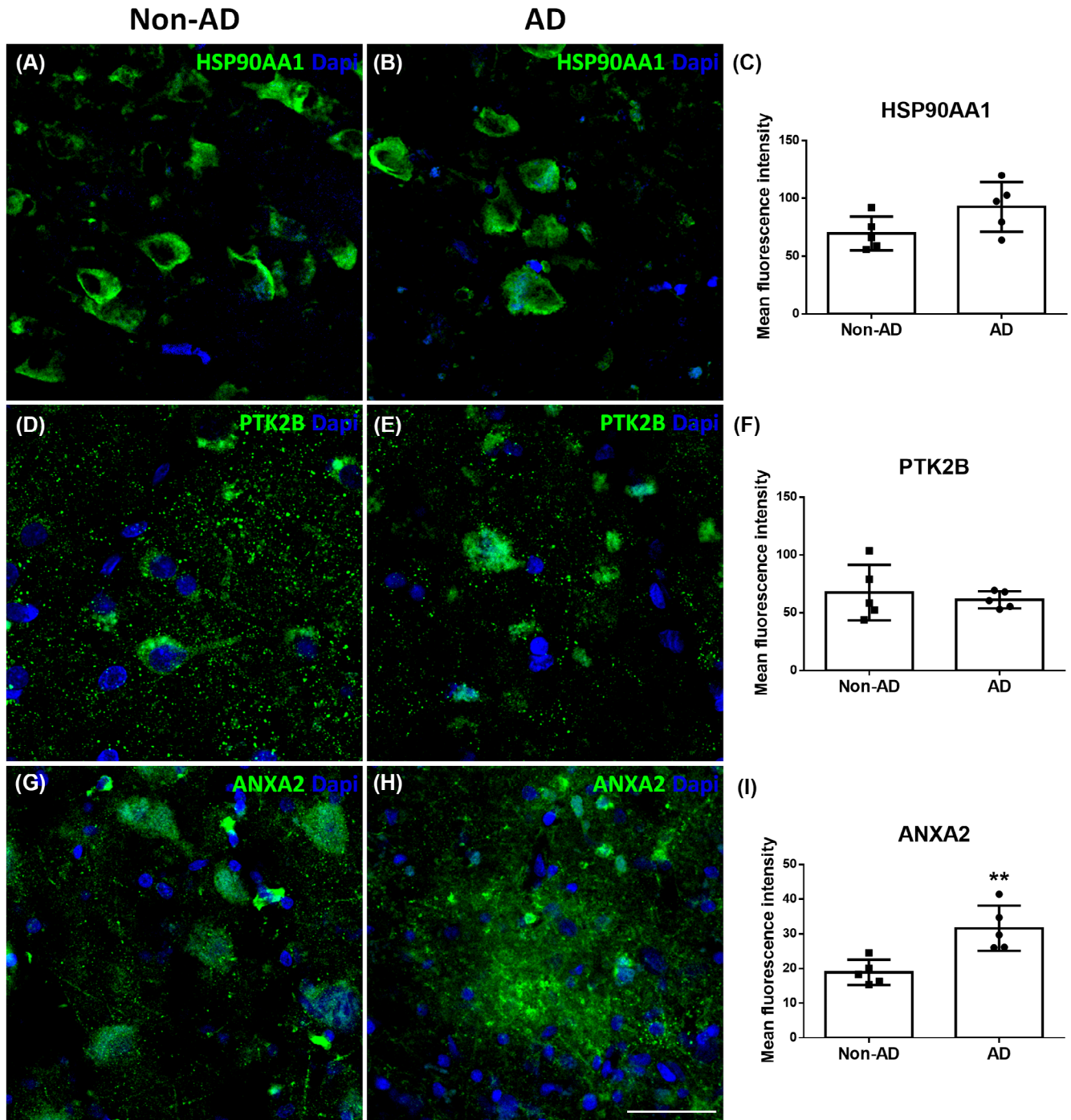


FIGURE 2 Validation of proteomic results through immunofluorescence: HSP90AA1, PTK2B, and ANXA2. Coronal sections of the human EC stained for HSP90AA1 in non-AD (A) and AD (B) cases, PTK2B in non-AD (D) and AD (E) cases and ANXA2 in non-AD (G) and AD (H) cases. Quantification from confocal fluorescence microscopy images of HSP90AA1 (C), PTK2B (F) and ANXA2 (I). The graphs show the mean \pm SD, ** p value < 0.01 . Scale bar = 40 μ m for (A,B) and (G,H) and 25 μ m for (D,E). AD, Alzheimer's disease; EC, entorhinal cortex.

HSP90AA1, PTK2B, and ANXA2 colocalize with glial cells (astroglia and/or microglia) provides additional support for the role of innate immune responses in the central nervous system in AD progression, and the relationship of these immune responses to A β and tau pathology.

To better characterize the relevance of DEPs and their implications for the pathology of AD, a

bioinformatic analysis of human EC proteomic data was performed. A total of 139 significant DEPs (52 upregulated and 87 downregulated) were identified, and the most altered signaling pathway in the EC of AD cases was synaptogenesis (Figure 1A–C). SYNGO analysis revealed 37 DEPs involved in synapse function, where PTK2B was affected both presynaptically and

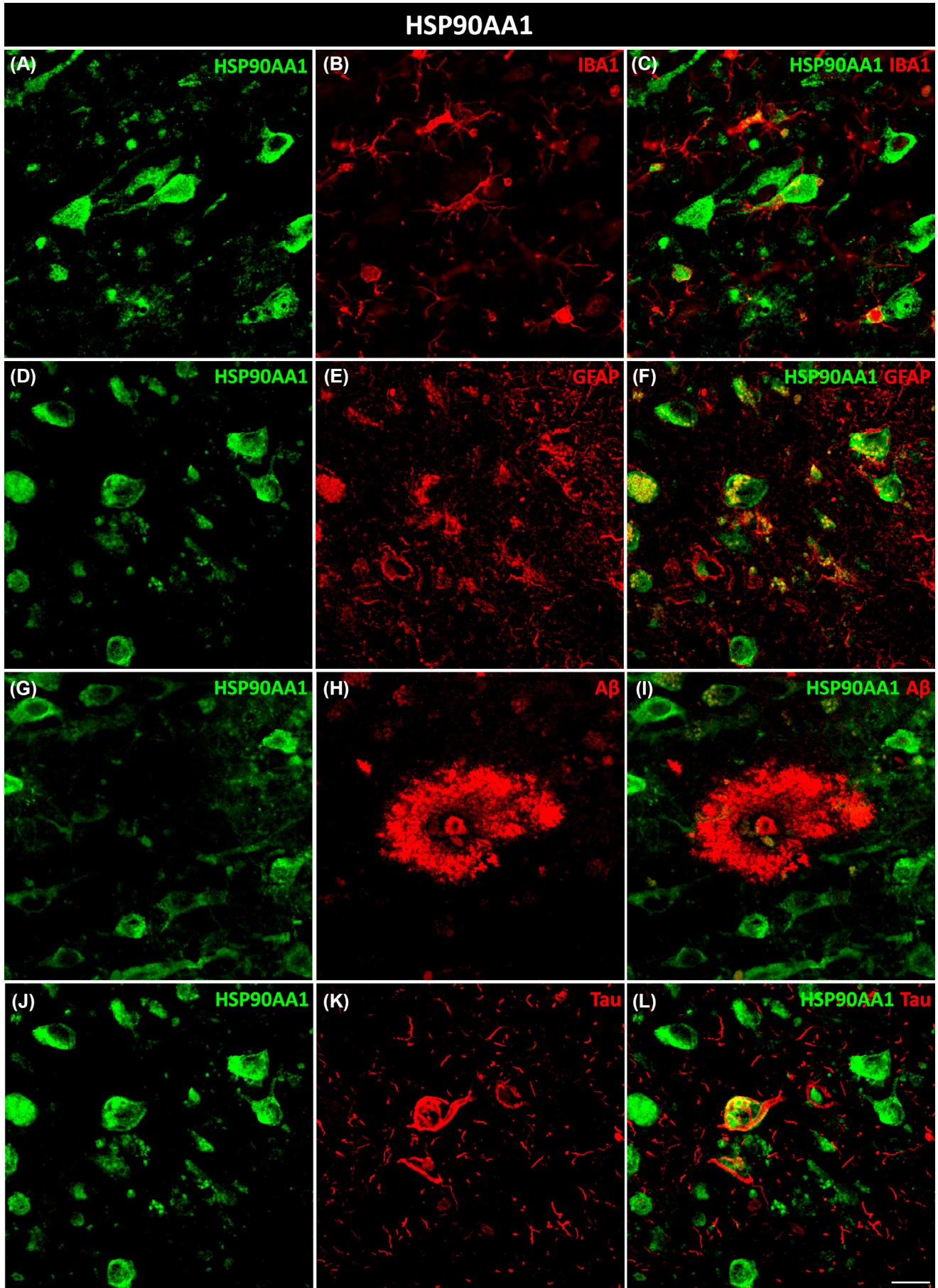


FIGURE 3 Legend on next page.

postsynaptically (Dataset S1d,f). We also evaluated the existence of an association between DEPs and pathological A β (APP) and tau (MAPT) proteins, where ANXA2 was related to A β , PTK2B was related to tau, and HSP90AA1 was related to both (Figure 1D). Furthermore, HSP90AA1, PTK2B, and ANXA2 displayed direct and indirect interactions with APP and AIF1 (synonyms of IBA1) in the interactome map based on pathway analysis (Figure 1E). According to proteomic and bioinformatic analyses, two downregulated proteins, HSP90AA1 and PTK2B, and one upregulated protein, ANXA2, were selected as the DEPs of interest for western blot, immunofluorescence, and confocal studies (Figure S1 and Figure 2). Finally, we carefully examined the expression patterns of these proteins in neurons, astroglia, and microglia to disentangle cell-type-specific relations to disease pathology (Figures 3–7).

The results revealed that synaptic homeostasis was disrupted, specifically at the synaptogenesis level, with a marked decrease in the growth and branching functions of dendrites and axons (Figure 1A–C). This would lead to neurodegeneration, which is widely described in AD [17, 18]. Synaptic pathology occurs early in AD and has been correlated with cognitive impairment [26]. However, the molecular mechanisms that lead to synaptic dysfunction remain unclear. Most research focuses on the harmful consequences of soluble toxic forms of A β and tau at synapses [27, 28]. For this reason, we constructed a Venn diagram of DEPs related to A β (APP) and tau (MAPT), where PTK2B was related to tau, ANXA2 was related to A β , and HSP90AA1 was related to both (Figure 1D). In a representative interactome map of functional relationships, the central node, APP, was linked to different proteins, including HSP90AA1, PTK2B, and ANXA2 (Figure 1E). Notably, the network revealed indirect relationships with AIF1, which is related to microglial cells. Glia-mediated neuroinflammation is also involved in synaptic dysfunction [5, 28]. In particular, recent research findings suggest that microglia and astroglia might contribute to synapse loss by engulfing synaptic structures [28]. Microglia and astroglia have recently been considered crucial players in the pathology of AD, but their protective or harmful roles remain unclear [5]. Evidence suggests that both populations could be involved in either the clearance or, conversely, the spread of A β and tau pathological proteins [6–9]. One of the main goals of this study was to characterize the contribution of HSP90AA1, PTK2B, and ANXA2 to neurons, microglia, and astroglia and the spatial relationships with A β and tau in the EC in AD (Figures 3–5, respectively).

HSP90 is an essential chaperone that regulates proper protein folding in the cell [29]. Two main subtypes are expressed in mammals: HSP90 β (HSP90AB1), which is constitutively expressed, and HSP90 α (HSP90AA1), which is enriched in the brain and acts as an inducible molecular chaperone that participates in the stress response [29, 30]. In cooperation with its cochaperones, HSP90 is capable of regulating tau phosphorylation and dephosphorylation [30]. In fact, HSP90AA1 was found to colocalize with tau protein (Figure 3L). Several lines of investigation support the idea that the inhibition of HSP90 is a promising way to reduce tau pathology [31–33]. Hsp90 was found to promote A β clearance through the activation of microglial phagocytosis in AD [29, 30, 33, 34]. HSP90AA1 is also considered a microglial activation marker in Parkinson's disease [35]. In our study, HSP90AA1 colocalized with microglia (Figure 3C) and was distributed around A β plaques (Figure 3I). Moreover, we demonstrated for the first time that HSP90AA1 colocalized with astrocytes (Figure 3F). This interaction should be further studied to elucidate its role in AD.

PTK2B is a nonreceptor cytoplasmic tyrosine kinase predominantly expressed in neurons [36], and its colocalization pattern was verified in this study (Figure 4C). It plays an important role in synaptic function and is involved in NMDA receptor regulation, hippocampus-related memory, dendritic spine structure modulation, postsynaptic organization, and synaptic plasticity [37]. This is in accordance with our SYNGO results, which showed that PTK2B was involved in synaptic function and was affected in both pre- and postsynapses (Dataset S1f). Regarding pathological proteins, our results showed a colocalization of PTK2B with both A β and tau proteins in the EC in AD (Figure 4I,L). PTK2B accumulation represents an early pathological marker corresponding to progressive pathological stages of tau in AD patients and in transgenic mice [38]. In fact, hyperphosphorylated tau was found to colocalize with PTK2B in the human AD brain [38]. GSK3 β , the main kinase phosphorylating tau protein, is activated by PTK2B [39, 40]. Additional investigations revealed that PTK2B could act as a direct tyrosine kinase of tau [41]. PTK2B activity displays differing effects on A β and tau in the sense that PTK2B mediates toxic A β signaling but suppresses tau phosphorylation, protecting against tauopathy in AD [40]. We have shown for the first time that PTK2B is also expressed in microglial cells in the EC in AD (Figure 4F). This protein seems to be required for normal macrophage polarization and migration toward sites of inflammation [42].

FIGURE 3 Glial and pathological colocalization of HSP90AA1. Double immunofluorescence staining of coronal sections of the human EC stained for HSP90AA1 and IBA1 for microglia (A–C), GFAP for astrocytes (D–F), A β (G–I), and tau (J–L) in AD cases. Scale bar = 20 μ m. A β , amyloid- β ; AD, Alzheimer's disease; EC, entorhinal cortex.

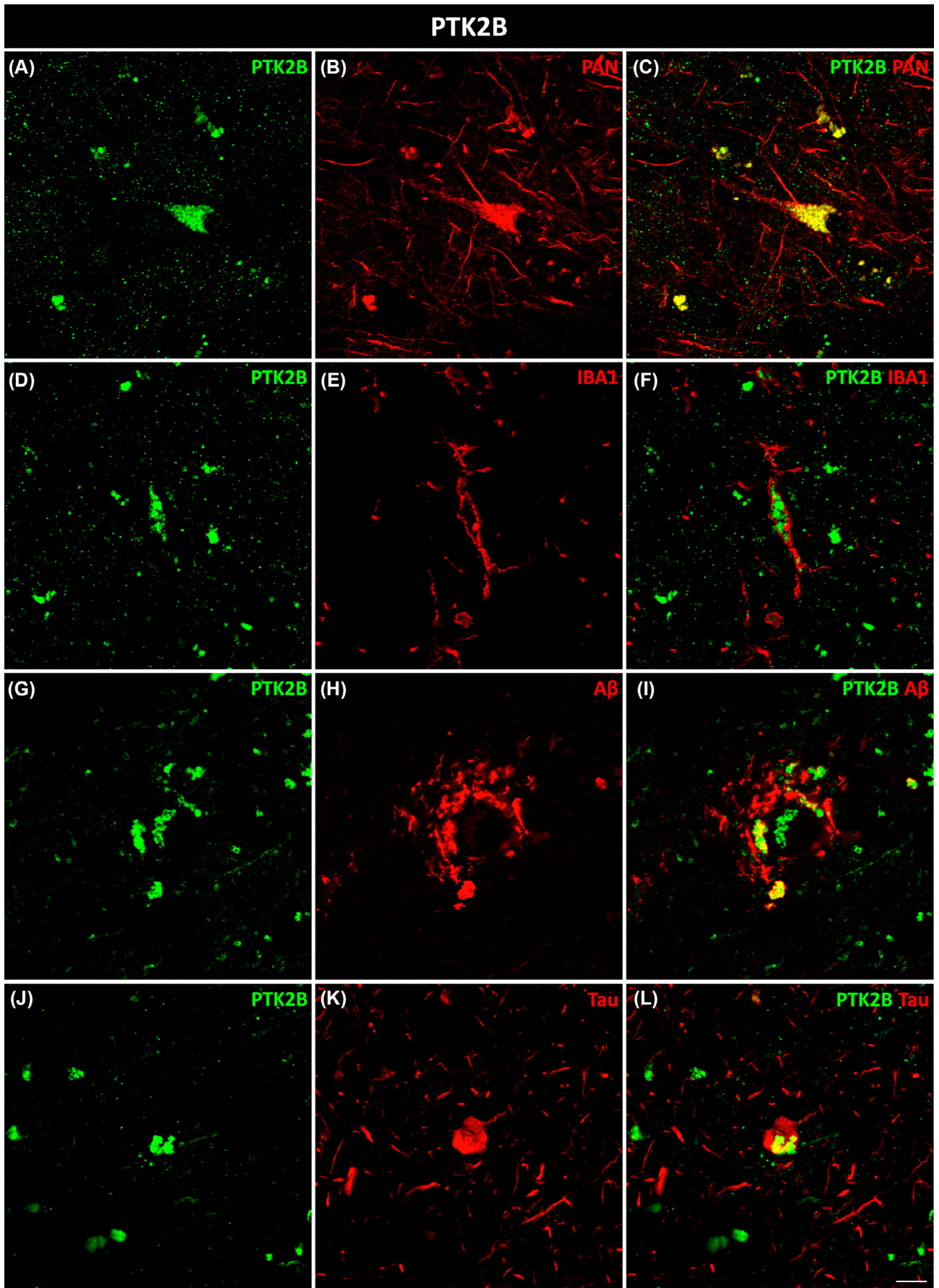


FIGURE 4 Legend on next page.

ANXA2, a calcium-regulated membrane-binding protein, is present in the growth cones and axonal branches of neurons [43]. Knowledge of the involvement of ANXA2 in the pathology of AD is limited. It has been identified as a tau-interacting protein [44]. The tau–ANXA2 interaction could retain tau protein in the axonal compartment of neurons [45]. ANXA2 was found in the present study to be upregulated in the EC in AD, which could control the mislocalization of tau. This could point to a compensatory mechanism of the affected neurons in patients. Concerning A β , one study implicated ANXA2 as a regulator of A β metabolism, facilitating autophagosome–lysosome fusion to decrease A β [46]. A recent investigation of the human amygdala revealed that ANXA2, whose abundance was increased in AD samples, was colocalized with A β plaques [47]. In this study, ANXA2 showed an intense spatial relationship with A β plaques in the EC in AD (Figure 5I). Remarkably, astrocytes were located around A β plaques that coexpressed ANXA2 (Figure 6). Therefore, the presence of ANXA2 could be involved in astroglia containing A β plaques. Regarding glial cells, our results showed colocalization of ANXA2 with both astroglia and microglia in the EC in AD (Figure 5C,F). A single study showed that ANXA2 was expressed by reactive astrocytes (identified by a prominent cytoplasm and processes with strong GFAP immunoreactivity) in the human hippocampus, whereas quiescent astrocytes were minimally immunoreactive [48]. On the other hand, ANXA2 has been linked to A β -mediated microglial activation and proinflammatory responses through tissue plasminogen activator (tPA) signaling pathways, which produce plasmin to degrade A β peptides [49]. Interestingly, triple colocalization of ANXA2, HSP90AA1, and IBA1 was observed specifically in amoeboid microglia (Figure 7), which is indicative of activated microglia, in contrast to the resting ramified morphology [50]. Therefore, the interaction of ANXA2 and HSP90AA1 could be necessary to activate microglia toward their phagocytic form to degrade A β deposits.

All three proteins investigated in this study showed a relationship with microglial cells. It has been reported that microglia show different states during the course of AD. Microglia have a beneficial role at the beginning of the disease, limiting the toxic accumulation of A β and tau through clearance or phagocytosis [5, 7, 51] or compacting and corralling A β plaques [52]. However, there is also considerable evidence supporting that activated microglia can be harmful in AD progression [5, 51], becoming unable to protect against the A β burden and exacerbating tau pathology [10, 53]. Additionally, microglia can

directly cause synaptic loss through the engulfment and removal of synapses and can secrete proinflammatory factors that can damage neurons either directly or indirectly by activating neurotoxic astrocytes [28, 51, 54–56]. In particular, it has been shown that reactive astrocyte subtype A1 is induced by activated microglia and causes the astrocytes to lose many astrocytic functions, such as support for neurons, synapse formation, and pruning of synapses and myelin debris by phagocytosis [54, 57]. Furthermore, A1 astrocytes secrete a neurotoxin that leads to the death of neurons and oligodendrocytes [54]. This suggests that A1 astrocytes, induced by activated microglia, are toxic to the synapse and that their presence could contribute to neurodegeneration and disease progression.

Taken together, the evidence suggests that unbalanced expression of HSP90AA1, PTK2B, and ANXA2 could contribute to synaptic decline in AD by acting on microglial cells as follows (Figure 8): HSP90AA1 downregulation could decrease microglial activation and A β clearance; PTK2B, also downregulated, could reduce the polarization and migration of microglia to A β deposits in synaptic structures; ANXA2 upregulation could promote A β -mediated microglial activation and subsequently induce A β degradation and activate neurotoxic astrocytes, pointing to a dual neuroprotective and neurotoxic role of ANXA2. As a result, synaptic homeostasis could be disrupted, with a marked decrease in the growth and branching of dendrites and axons. Collectively, these findings suggest the relevance of microglial cells in the propagation of neurodegenerative and neuroinflammatory processes in AD.

5 | CONCLUSIONS

In conclusion, this report implicates synaptogenesis as the most disrupted signaling pathway in the human EC in AD, and HSP90AA1, PTK2B, and ANXA2 proteins are highlighted as key factors that could aggravate synaptic decline via microglia. Notably, ANXA2 could also be involved in the containment of A β plaques by astroglial cells. Therefore, a better understanding of microglia–synapse signaling events and astroglia–A β burden is needed to prevent synaptic dysfunction, neurodegeneration, and cognitive decline. Moreover, an analysis of human cases in early or intermediate stages of the disease would allow to further research the glial responses to the progression of AD pathology. This information would be helpful in elucidating AD pathogenesis, thus improving diagnostics and therapeutics for AD.

FIGURE 4 Neuronal, microglial, and pathological colocalization of PTK2B. Double immunofluorescence staining of coronal sections of the human EC stained for PTK2B and PAN for neurons in non-AD cases (A–C) and IBA1 for microglia (D–F), A β (G–I), and tau (J–L) in AD cases. Scale bar = 10 μ m. AD, Alzheimer's disease; EC, entorhinal cortex.

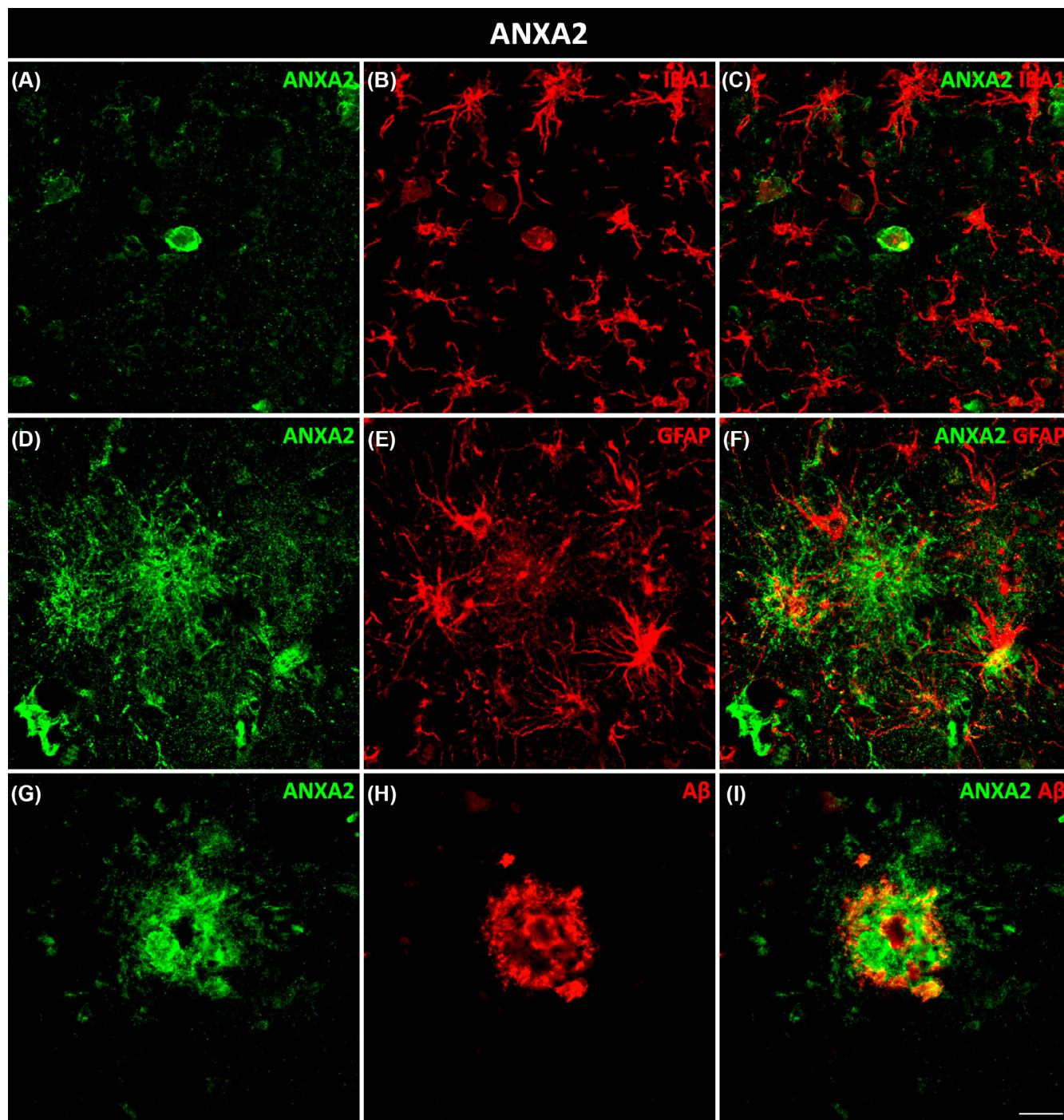


FIGURE 5 Glial and pathological colocalization of ANXA2. Double immunofluorescence staining of coronal sections of the human EC stained for ANXA2 and IBA1 for microglia (A–C), GFAP for astrocytes (D–F), and A β (G–I) in AD cases. Scale bar = 20 μ m. EC, entorhinal cortex.

AUTHOR CONTRIBUTIONS

VAL, IUB and AFC contributed to experimental design and data collection; VAL, SVC and MGR performed the experiments and analyzed data; VAL and DSS contributed to interpretation of the proteomic data and statistical analysis; VAL and AMM wrote the manuscript. All authors read and approved the final manuscript.

ACKNOWLEDGMENTS

We are particularly grateful for the generous contribution of the patients and the collaboration of *Institut d'Investigacions Biomèdiques August Pi i Sunyer (IDIBAPS)*, *Biobanco en Red de la Región de Murcia (BIOBANC-MUR)*, *Biobanco de Tejidos de la Fundación CIEN (BTCIEN)*, and *Biobanco del Principado de Asturias (BPA)*, registered on the *Registro Nacional de Biobancos*. In addition, the

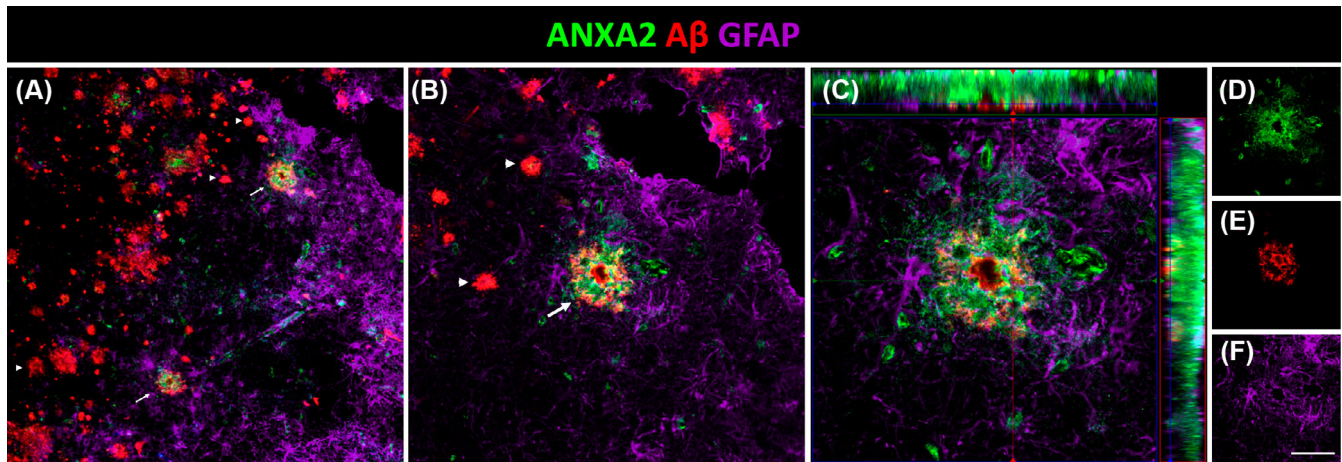


FIGURE 6 Triple colocalization of ANXA2, A β plaques and astrocytes in AD. (A) Coronal section of the human EC immunofluorescently stained for ANXA2, A β and GFAP for astrocytes and detail (B). Arrows and arrowheads indicate A β plaques with and without ANXA2, respectively. Orthogonal view of the z-stack (C) and each of its channels in green ANXA2 (D), red A β (E), and purple astrocytes (F). Scale bars for A = 70 μ m, B = 35 μ m, C = 20 μ m, and D–F = 55 μ m. A β , amyloid- β ; AD, Alzheimer's disease; EC, entorhinal cortex.

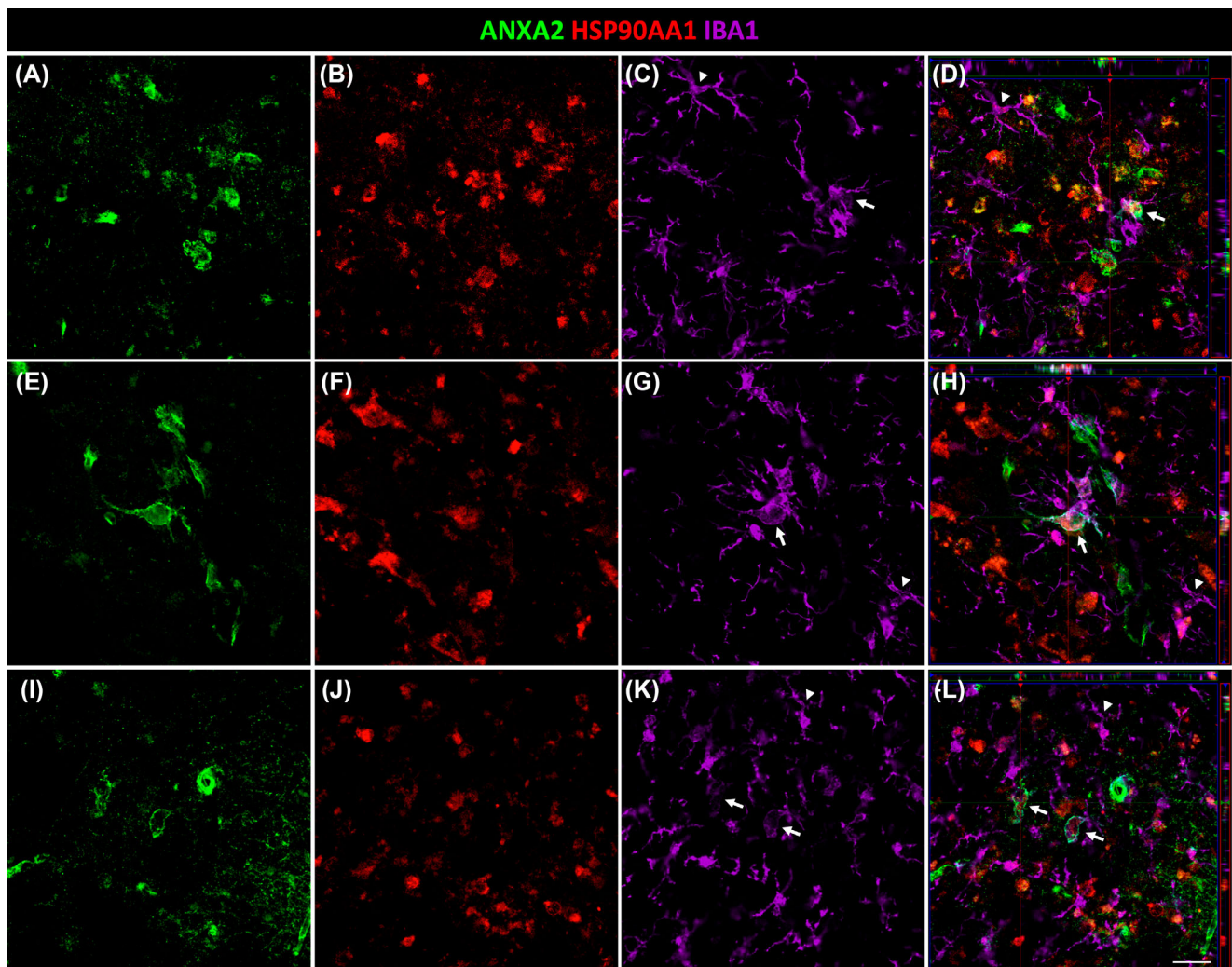


FIGURE 7 Triple colocalization of ANXA2, HSP90AA1, and microglia in AD. Coronal sections of the human EC immunofluorescently stained for ANXA2 (A, E, I), HSP90AA1 (B, F, J), and IBA1 (C, G, K) for microglia. Orthogonal views of corresponding z-stacks (D, H, L). Each z-stack corresponds to a specific number of slices. Arrows and arrowheads indicate amoeboid and ramified microglia, respectively. Scale bar = 20 μ m.

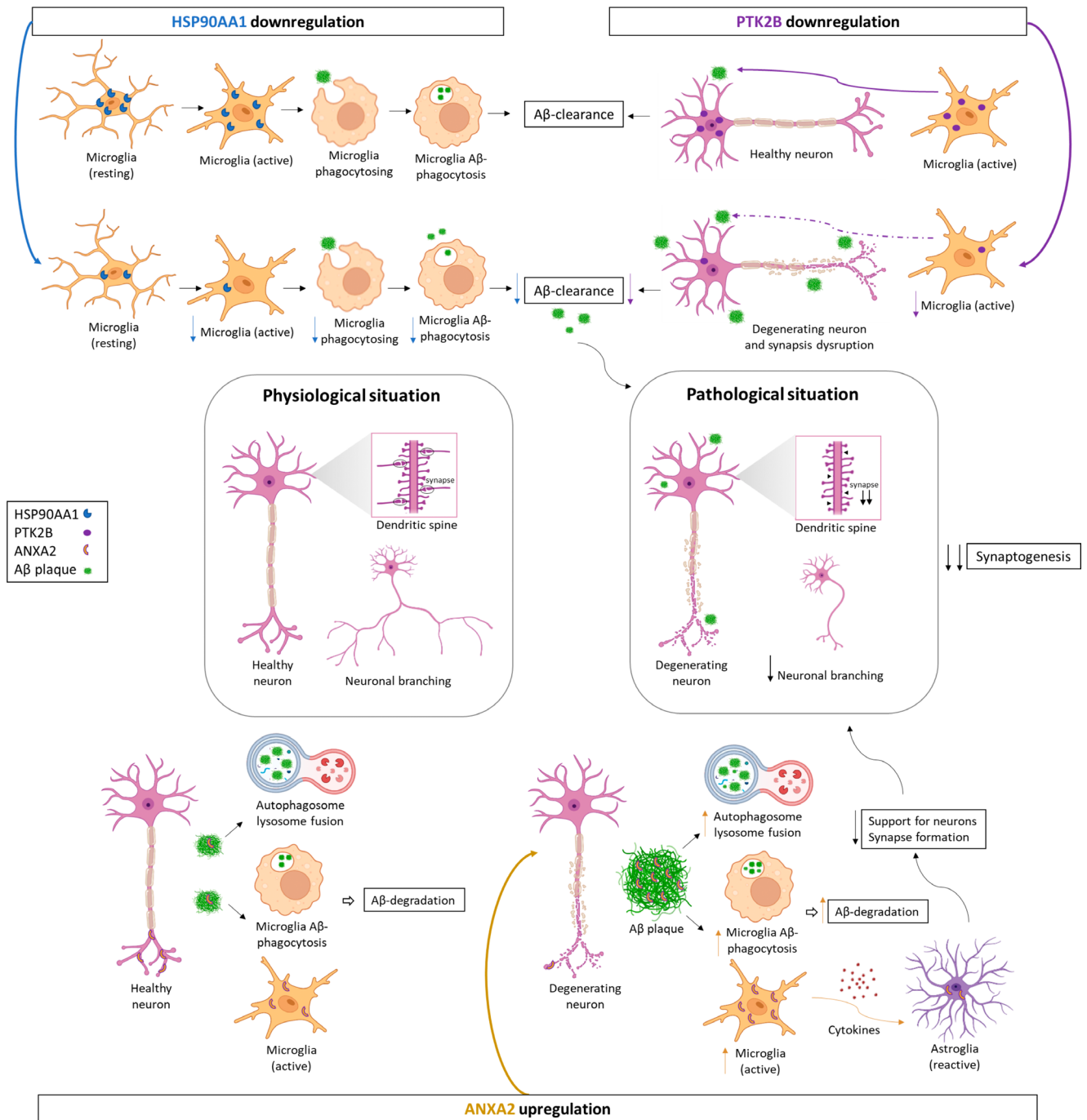


FIGURE 8 Potential role of HSP90AA1, PTK2B, and ANXA2 in synaptic decline through microglial cells in AD. HSP90AA1 promotes Aβ clearance through activation of microglial phagocytosis in AD. Its downregulation decreases microglial activation, phagocytosis, and consequently Aβ clearance at synapses. PTK2B, expressed in neurons, promotes normal macrophage polarization and migration to inflamed areas in synaptic structures. However, PTK2B is downregulated, and consequently, microglial cell activation and migration to Aβ deposits are reduced, contributing to neurodegeneration and synapse disruption. ANXA2, present in neurons as well, could contain Aβ pathology through autophagosome-lysosome fusion and the activation of microglial cells. Therefore, its upregulation could increase autophagosome-lysosome fusion and Aβ-mediated microglial activation and subsequently promote Aβ degradation. On the other hand, active microglia secrete proinflammatory cytokines that can damage neurons either directly or indirectly by activating neurotoxic astrocytes. Additionally, ANXA2 is expressed in reactive astrocytes, which lose many normal astrocytic functions, including neuron support and synapse formation. As a result, it leads to the formation of fewer and weaker synapses and a decline in synaptogenesis. Therefore, synaptic homeostasis is disrupted with a marked decrease in the growth and branching of dendrites and axons, and neurodegeneration occurs in the EC of AD patients. Figure created with [BioRender.com](https://www.biorender.com). Aβ, amyloid-β; AD, Alzheimer's disease; EC, entorhinal cortex.

experiments were carried out in the facilities of the Ciudad Real Medical School UCAI. This work is part of the doctoral thesis of Veronica Astillero Lopez.

FUNDING INFORMATION

Sponsored by the UCLM/ERDF (2022-GRIN-34200 to N. P. N. D.), the Spanish Ministry of Science and

Innovation (grant no. PID2019-108659RB-I00 to A. M.-M.), and the Autonomous Government of Castilla-La Mancha/ERDF (grant no. SBPLY/17/180501/000430 to A. M.-M. and D.S.-S. and SBPLY/21/180501/000093 to A. M.-M. and I. U.-B). S.V.-C. and M.G.-R. held predoctoral fellowships granted by UCLM/ESF.

CONFLICT OF INTEREST STATEMENT

The authors declare no conflicts of interest.

DATA AVAILABILITY STATEMENT

The datasets analyzed during the current study are available in the ProteomeXchange Consortium (<http://proteomecentral.proteomexchange.org>) via the PRIDE partner repository with the dataset identifier PXD029359 (Username: reviewer_pxd029359@ebi.ac.uk; Password: 9ZBBqh6c). The data supporting the findings of this study are available in Supplementary Material. Raw data are available from the corresponding author, upon reasonable request.

ETHICS STATEMENT

Postmortem human brain samples were collected and processed following standard operating procedures with the approval of the Clinical Research Ethics Committee of Ciudad Real University Hospital (PID2019-108659RBI00). These processes included obtaining the donors' written consent.

PERMISSION TO REPRODUCE MATERIAL FROM OTHER SOURCES

The authors have obtained the corresponding permissions from other sources such as Biorender.

CLINICAL TRIAL REGISTRATION

Not applicable.

ORCID

Isabel Ubeda-Banon  <https://orcid.org/0000-0003-1753-5469>

Daniel Saiz-Sanchez  <https://orcid.org/0000-0001-7002-8031>

Alino Martinez-Marcos  <https://orcid.org/0000-0003-3691-3605>

REFERENCES

- Scheltens P, De Strooper B, Kivipelto M, Holstege H, Chetelat G, Teunissen CE, et al. Alzheimer's disease. *Lancet*. 2021;397(10284):1577–90.
- Vinters HV. Emerging concepts in Alzheimer's disease. *Annu Rev Pathol*. 2015;10:291–319.
- Prusiner SB. Cell biology. A unifying role for prions in neurodegenerative diseases. *Science*. 2012;336(6088):1511–3.
- Peng C, Trojanowski JQ, Lee VM. Protein transmission in neurodegenerative disease. *Nat Rev Neurol*. 2020;16(4):199–212.
- Henstridge CM, Hyman BT, Spires-Jones TL. Beyond the neuron-cellular interactions early in Alzheimer disease pathogenesis. *Nat Rev Neurosci*. 2019;20(2):94–108.
- Martini-Stoica H, Cole AL, Swartzlander DB, Chen F, Wan YW, Bajaj L, et al. TFEB enhances astroglial uptake of extracellular tau species and reduces tau spreading. *J Exp Med*. 2018;215(9):2355–77.
- Bolos M, Llorens-Martin M, Jurado-Arjona J, Hernandez F, Rabano A, Avila J. Direct evidence of internalization of tau by microglia in vitro and in vivo. *J Alzheimers Dis*. 2016;50(1):77–87.
- Narasimhan S, Changolkar L, Riddle DM, Kats A, Stieber A, Weitzman SA, et al. Human tau pathology transmits glial tau aggregates in the absence of neuronal tau. *J Exp Med*. 2020;217(2):e20190783.
- Venegas C, Kumar S, Franklin BS, Dierkes T, Brinkschulte R, Tejera D, et al. Microglia-derived ASC specks cross-seed amyloid-beta in Alzheimer's disease. *Nature*. 2017;552(7685):355–61.
- Krabbe G, Halle A, Matyash V, Rinnenthal JL, Eom GD, Bernhardt U, et al. Functional impairment of microglia coincides with Beta-amyloid deposition in mice with Alzheimer-like pathology. *PLoS One*. 2013;8(4):e60921.
- Braak H, Alafuzoff I, Arzberger T, Kretschmar H, Del Tredici K. Staging of Alzheimer disease-associated neurofibrillary pathology using paraffin sections and immunocytochemistry. *Acta Neuropathol*. 2006;112(4):389–404.
- Witter MP. The perforant path: projections from the entorhinal cortex to the dentate gyrus. *Prog Brain Res*. 2007;163:43–61.
- Ubeda-Banon I, Saiz-Sanchez D, Flores-Cuadrado A, Rioja-Corroto E, Gonzalez-Rodriguez M, Villar-Conde S, et al. The human olfactory system in two proteinopathies: Alzheimer's and Parkinson's diseases. *Transl Neurodegener*. 2020;9(1):22.
- Qasim SE, Miller J, Inman CS, Gross RE, Willie JT, Lega B, et al. Memory retrieval modulates spatial tuning of single neurons in the human entorhinal cortex. *Nat Neurosci*. 2019;22(12):2078–86.
- Squire LR, Stark CE, Clark RE. The medial temporal lobe. *Annu Rev Neurosci*. 2004;27:279–306.
- Pini L, Pievani M, Bocchetta M, Altomare D, Bosco P, Cavedo E, et al. Brain atrophy in Alzheimer's disease and aging. *Ageing Res Rev*. 2016;30:25–48.
- Gomez-Isla T, Hollister R, West H, Mui S, Growdon JH, Petersen RC, et al. Neuronal loss correlates with but exceeds neurofibrillary tangles in Alzheimer's disease. *Ann Neurol*. 1997;41(1):17–24.
- Astillero-Lopez V, Gonzalez-Rodriguez M, Villar-Conde S, Flores-Cuadrado A, Martinez-Marcos A, Ubeda-Banon I, et al. Neurodegeneration and astrogliosis in the entorhinal cortex in Alzheimer's disease: stereological layer-specific assessment and proteomic analysis. *Alzheimers Dement*. 2022;18(12):2468–80.
- Xu J, Patassini S, Rustogi N, Riba-Garcia I, Hale BD, Phillips AM, et al. Regional protein expression in human Alzheimer's brain correlates with disease severity. *Commun Biol*. 2019;2:43.
- Li KW, Ganz AB, Smit AB. Proteomics of neurodegenerative diseases: analysis of human post-mortem brain. *J Neurochem*. 2019;151(4):435–45.
- Mendonca CF, Kuras M, Nogueira FCS, Pla I, Hortobagyi T, Csiba L, et al. Proteomic signatures of brain regions affected by tau pathology in early and late stages of Alzheimer's disease. *Neurobiol Dis*. 2019;130:104509.
- Gonzalez-Rodriguez M, Villar-Conde S, Astillero-Lopez V, Villanueva-Anguita P, Ubeda-Banon I, Flores-Cuadrado A, et al. Neurodegeneration and astrogliosis in the human CA1 hippocampal subfield are related to hsp90ab1 and bag3 in Alzheimer's disease. *Int J Mol Sci*. 2021;23(1):165.
- Ferrer I, Andres-Benito P, Ausin K, Pamplona R, Del Rio JA, Fernandez-Irigoyen J, et al. Dysregulated protein phosphorylation: a determining condition in the continuum of brain aging and Alzheimer's disease. *Brain Pathol*. 2021;31(6):e12996.
- Jia Y, Wang X, Chen Y, Qiu W, Ge W, Ma C. Proteomic and transcriptomic analyses reveal pathological changes in the entorhinal cortex region that correlate well with dysregulation of ion

- transport in patients with Alzheimer's disease. *Mol Neurobiol.* 2021;58(8):4007–27.
25. Mai JK, Paxinos G, Voss T. Atlas of the human brain. 3rd ed. San Diego, CA: Elsevier Science; 2008.
 26. DeKosky ST, Scheff SW. Synapse loss in frontal cortex biopsies in Alzheimer's disease: correlation with cognitive severity. *Ann Neurol.* 1990;27(5):457–64.
 27. Spires-Jones TL, Hyman BT. The intersection of amyloid beta and tau at synapses in Alzheimer's disease. *Neuron.* 2014;82(4):756–71.
 28. Griffiths J, Grant SGN. Synapse pathology in Alzheimer's disease. *Semin Cell Dev Biol.* 2023;139:13–23.
 29. Ou JR, Tan MS, Xie AM, Yu JT, Tan L. Heat shock protein 90 in Alzheimer's disease. *Biomed Res Int.* 2014;2014:796869.
 30. Bohush A, Bieganowski P, Filipek A. Hsp90 and its co-chaperones in neurodegenerative diseases. *Int J Mol Sci.* 2019;20(20):4976.
 31. Lee VM, Brunden KR, Hutton M, Trojanowski JQ. Developing therapeutic approaches to tau, selected kinases, and related neuronal protein targets. *Cold Spring Harb Perspect Med.* 2011;1(1):a006437.
 32. Blair LJ, Sabbagh JJ, Dickey CA. Targeting Hsp90 and its co-chaperones to treat Alzheimer's disease. *Expert Opin Ther Targets.* 2014;18(10):1219–32.
 33. Campanella C, Pace A, Caruso Bavisotto C, Marzullo P, Marino Gammazza A, Buscemi S, et al. Heat shock proteins in Alzheimer's disease: role and targeting. *Int J Mol Sci.* 2018;19(9):2603.
 34. Zhang M, Qian C, Zheng ZG, Qian F, Wang Y, Thu PM, et al. Jujuboside a promotes A β clearance and ameliorates cognitive deficiency in Alzheimer's disease through activating Axl/HSP90/PPAR γ pathway. *Theranostics.* 2018;8(15):4262–78.
 35. Smajic S, Prada-Medina CA, Landoulsi Z, Ghelfi J, Delcambre S, Dietrich C, et al. Single-cell sequencing of human midbrain reveals glial activation and a Parkinson-specific neuronal state. *Brain.* 2022;145(3):964–78.
 36. Menegon A, Burgaya F, Baudot P, Dunlap DD, Girault JA, Valtorta F. FAK+ and PYK2/CAKbeta, two related tyrosine kinases highly expressed in the central nervous system: similarities and differences in the expression pattern. *Eur J Neurosci.* 1999; 11(11):3777–88.
 37. Giralt A, Brito V, Chevy Q, Simonnet C, Otsu Y, Cifuentes-Diaz C, et al. Pyk2 modulates hippocampal excitatory synapses and contributes to cognitive deficits in a Huntington's disease model. *Nat Commun.* 2017;8:15592.
 38. Dourlen P, Fernandez-Gomez FJ, Dupont C, Grenier-Boley B, Bellenguez C, Obriot H, et al. Functional screening of Alzheimer risk loci identifies PTK2B as an in vivo modulator and early marker of tau pathology. *Mol Psychiatry.* 2017;22(6):874–83.
 39. Sayas CL, Avila J. GSK-3 and tau: a key duet in Alzheimer's disease. *Cell.* 2021;10(4):721.
 40. Brody AH, Nies SH, Guan F, Smith LM, Mukherjee B, Salazar SA, et al. Alzheimer risk gene product Pyk2 suppresses tau phosphorylation and phenotypic effects of tauopathy. *Mol Neurodegener.* 2022;17(1):32.
 41. Li C, Gotz J. Pyk2 is a novel tau tyrosine kinase that is regulated by the tyrosine kinase Fyn. *J Alzheimers Dis.* 2018;64(1):205–21.
 42. Okigaki M, Davis C, Falasca M, Harroch S, Felsenfeld DP, Sheetz MP, et al. Pyk2 regulates multiple signaling events crucial for macrophage morphology and migration. *Proc Natl Acad Sci U S A.* 2003;100(19):10740–5.
 43. Zhao WQ, Lu B. Expression of annexin A2 in GABAergic interneurons in the normal rat brain. *J Neurochem.* 2007;100(5):1211–23.
 44. Gauthier-Kemper A, Weissmann C, Golovyashkina N, Sebo-Lemke Z, Drewes G, Gerke V, et al. The frontotemporal dementia mutation R406W blocks tau's interaction with the membrane in an annexin A2-dependent manner. *J Cell Biol.* 2011;192(4): 647–61.
 45. Gauthier-Kemper A, Suarez Alonso M, Sundermann F, Niewidok B, Fernandez MP, Bakota L, et al. Annexins A2 and A6 interact with the extreme N terminus of tau and thereby contribute to tau's axonal localization. *J Biol Chem.* 2018;293(21): 8065–76.
 46. Bustos V, Pulina MV, Bispo A, Lam A, Flajolet M, Gorelick FS, et al. Phosphorylated presenilin 1 decreases beta-amyloid by facilitating autophagosome-lysosome fusion. *Proc Natl Acad Sci U S A.* 2017;114(27):7148–53.
 47. Gonzalez-Rodriguez M, Villar-Conde S, Astillero-Lopez V, Villanueva-Anguita P, Ubeda-Banon I, Flores-Cuadrado A, et al. Human amygdala involvement in Alzheimer's disease revealed by stereological and dia-PASEF analysis. *Brain Pathol.* 2023;33: e13180.
 48. Eberhard DA, Brown MD, VandenBerg SR. Alterations of annexin expression in pathological neuronal and glial reactions. Immunohistochemical localization of annexins I, II (p36 and p11 subunits), IV, and VI in the human hippocampus. *Am J Pathol.* 1994;145(3):640–9.
 49. Pineda D, Ampurdanes C, Medina MG, Serratosa J, Tusell JM, Saura J, et al. Tissue plasminogen activator induces microglial inflammation via a noncatalytic molecular mechanism involving activation of mitogen-activated protein kinases and Akt signaling pathways and AnnexinA2 and Galectin-1 receptors. *Glia.* 2012; 60(4):526–40.
 50. Lier J, Streit WJ, Bechmann I. Beyond activation: characterizing microglial functional phenotypes. *Cell.* 2021;10(9):2236.
 51. Hansen DV, Hanson JE, Sheng M. Microglia in Alzheimer's disease. *J Cell Biol.* 2018;217(2):459–72.
 52. Condello C, Yuan P, Schain A, Grutzendler J. Microglia constitute a barrier that prevents neurotoxic protofibrillar A β 42 hotspots around plaques. *Nat Commun.* 2015;6:6176.
 53. Leyns CEG, Holtzman DM. Glial contributions to neurodegeneration in tauopathies. *Mol Neurodegener.* 2017;12(1):50.
 54. Liddelov SA, Guttenplan KA, Clarke LE, Bennett FC, Bohlen CJ, Schirmer L, et al. Neurotoxic reactive astrocytes are induced by activated microglia. *Nature.* 2017;541(7638):481–7.
 55. Rajendran L, Paolicelli RC. Microglia-mediated synapse loss in Alzheimer's disease. *J Neurosci.* 2018;38(12):2911–9.
 56. Piccioni G, Mango D, Saidi A, Corbo M, Nistico R. Targeting microglia-synapse interactions in Alzheimer's disease. *Int J Mol Sci.* 2021;22(5):2342.
 57. Liddelov S, Barres B. SnapShot: astrocytes in health and disease. *Cell.* 2015;162(5):1170–1170.e1.

SUPPORTING INFORMATION

Additional supporting information can be found online in the Supporting Information section at the end of this article.

How to cite this article: Astillero-Lopez V, Villar-Conde S, Gonzalez-Rodriguez M, Flores-Cuadrado A, Ubeda-Banon I, Saiz-Sanchez D, et al. Proteomic analysis identifies HSP90AA1, PTK2B, and ANXA2 in the human entorhinal cortex in Alzheimer's disease: Potential role in synaptic homeostasis and A β pathology through microglial and astroglial cells. *Brain Pathology.* 2024;34(4):e13235. <https://doi.org/10.1111/bpa.13235>